[CANCER RESEARCH 64, 5617–5623, August 15, 2004]

Cannabinoids Inhibit the Vascular Endothelial Growth Factor Pathway in Gliomas

Cristina Blázquez,[1] Luis González-Feria,[4] Luis Álvarez,[2] Amador Haro,[1] M. Llanos Casanova,[3] and Manuel Guzmán[1]

[1]Department of Biochemistry and Molecular Biology I, School of Biology, Complutense University; [2]Research Unit, La Paz University Hospital; [3]Project on Cellular and Molecular Biology and Gene Therapy, CIEMAT, Madrid, Spain; and [4]Department of Neurosurgery, University Hospital, Tenerife, Spain

ABSTRACT

Cannabinoids inhibit tumor angiogenesis in mice, but the mechanism of their antiangiogenic action is still unknown. Because the vascular endothelial growth factor (VEGF) pathway plays a critical role in tumor angiogenesis, here we studied whether cannabinoids affect it. As a first approach, cDNA array analysis showed that cannabinoid administration to mice bearing s.c. gliomas lowered the expression of various VEGF pathway-related genes. The use of other methods (ELISA, Western blotting, and confocal microscopy) provided additional evidence that cannabinoids depressed the VEGF pathway by decreasing the production of VEGF and the activation of VEGF receptor (VEGFR)-2, the most prominent VEGF receptor, in cultured glioma cells and in mouse gliomas. Cannabinoid-induced inhibition of VEGF production and VEGFR-2 activation was abrogated both *in vitro* and *in vivo* by pharmacological blockade of ceramide biosynthesis. These changes in the VEGF pathway were paralleled by changes in tumor size. Moreover, intratumoral administration of the cannabinoid Δ^9-tetrahydrocannabinol to two patients with glioblastoma multiforme (grade IV astrocytoma) decreased VEGF levels and VEGFR-2 activation in the tumors. Because blockade of the VEGF pathway constitutes one of the most promising antitumoral approaches currently available, the present findings provide a novel pharmacological target for cannabinoid-based therapies.

INTRODUCTION

To grow beyond minimal size, tumors must generate a new vascular supply for purposes of gas exchange, cell nutrition, and waste disposal (1–4). They do so by secreting proangiogenic cytokines that promote the formation of blood vessels. Vascular endothelial growth factor (VEGF; also known as VEGF-A) is considered the most important proangiogenic molecule because it is expressed abundantly by a wide variety of animal and human tumors and because of its potency, selectivity, and ability to regulate most and perhaps all of the steps in the angiogenic cascade (1–4). The best characterized VEGF receptors are two related receptor tyrosine kinases termed VEGF receptor (VEGFR)-1 (also known as Flt-1) and VEGFR-2 (also known as kinase domain region or Flk-1). Although VEGF binds to VEGFR-1 with higher affinity, numerous studies in cultured cells and laboratory animals have provided evidence that VEGFR-2 is the major mediator of the mitogenic, antiapoptotic, angiogenic, and permeability-enhancing effects of VEGF (1–4). Because overexpression of VEGF and VEGFR-2 is causally involved in the progression of many solid tumors, several strategies to inhibit VEGF signaling have been translated into clinical trials in cancer patients, including anti-VEGF and anti-VEGFR-2 antibodies, small VEGFR-2 inhibitors, and a soluble decoy VEGFR (5–8). In addition, clinical trials are being performed with a number of promising anticancer compounds such as Iressa and Herceptin that block proteins involved in the induction of the VEGF pathway (5, 8).

Received 12/16/03; revised 4/1/04; accepted 6/10/04.

Grant support: Fundación Científica de la Asociación Española Contra el Cáncer and Ministerio de Ciencia y Tecnología Grant SAF2003-00745.

The costs of publication of this article were defrayed in part by the payment of page charges. This article must therefore be hereby marked *advertisement* in accordance with 18 U.S.C. Section 1734 solely to indicate this fact.

Requests for reprints: Manuel Guzmán, Department of Biochemistry and Molecular Biology I, School of Biology, Complutense University, 28040 Madrid, Spain. Phone: 34-913944668; Fax: 34-913944672; E-mail: mgp@bbm1.ucm.es.

Cannabinoids, the active components of *Cannabis sativa* L. (marijuana), and their derivatives exert a wide array of effects by activating their specific G protein-coupled receptors CB_1 and CB_2, which are normally engaged by a family of endogenous ligands–the endocannabinoids (9, 10). Marijuana and its derivatives have been used in medicine for many centuries, and there is currently a renaissance in the study of the therapeutic effects of cannabinoids. Today, cannabinoids are approved to palliate the wasting and emesis associated with cancer and AIDS chemotherapy (11), and ongoing clinical trials are determining whether cannabinoids are effective agents in the treatment of pain (12), neurodegenerative disorders such as multiple sclerosis (13), and traumatic brain injury (14). In addition, cannabinoid administration to mice and/or rats induces the regression of lung adenocarcinomas (15), gliomas (16), thyroid epitheliomas (17), lymphomas (18), and skin carcinomas (19). These studies have also evidenced that cannabinoids display a fair drug safety profile and do not produce the generalized cytotoxic effects of conventional chemotherapies, making them potential antitumoral agents (20, 21).

Little is known, however, about the mechanism of cannabinoid antitumoral action *in vivo*. By modulating key cell signaling pathways, cannabinoids directly induce apoptosis or cell cycle arrest in different transformed cells *in vitro* (20). However, the involvement of these events in their antitumoral action *in vivo* is as yet unknown. More recently, immunohistochemical and functional analyses of the vasculature of gliomas (22) and skin carcinomas (19) have shown that cannabinoid administration to mice inhibits tumor angiogenesis. These findings prompted us to explore the mechanism by which cannabinoids impair angiogenesis of gliomas and, particularly, the possible impact of cannabinoids on the VEGF pathway. Here, we report that cannabinoid administration inhibits the VEGF pathway in cultured glioma cells, in glioma-bearing mice, and in two patients with glioblastoma multiforme. In addition, this effect may be mediated by ceramide, a sphingolipid second messenger implicated previously in cannabinoid signaling in glioma cells (23).

MATERIALS AND METHODS

Cannabinoids. The Δ^9-tetrahydrocannabinol was kindly given by Alfredo Dupetit (The Health Concept, Richelbach, Germany). JWH-133 was kindly given by Dr. John Huffman (Department of Chemistry, Clemson University, Clemson, SC; Ref. 24). WIN-55,212-2 and anandamide were from Sigma (St. Louis, MO). SR141716 and SR144528 were kindly given by Sanofi-Synthelabo (Montpellier, France). For *in vitro* incubations, cannabinoid agonists and antagonists were directly applied at a final DMSO concentration of 0.1–0.2% (v/v). For *in vivo* experiments, ligands were prepared at 1% (v/v) DMSO in 100 μl PBS supplemented with 5 mg/ml BSA. No significant influence of the vehicle was observed on any of the parameters determined.

Cell Culture. The rat C6 glioma (25), the human U373 MG astrocytoma (25), the mouse PDV.C57 epidermal carcinoma (19), and the human ECV304 bladder cancer epithelioma (22) were cultured as described previously. Human glioma cells were prepared from a glioblastoma multiforme (grade IV astrocytoma; Ref. 26). The biopsy was digested with collagenase (type Ia; Sigma) in DMEM at 37°C for 90 min, the supernatant was seeded in DMEM containing 15% FCS and 1 mM glutamine, cells were grown for 2 passages, and 24 h before the experiments, cells were transferred to 0.5%-serum DMEM. Cell viability was determined by trypan blue exclusion. Rat recombinant VEGF and *N*-acetylsphingosine (C_2-ceramide) were from Sigma.

Tumor Induction in Mice. Tumors were induced in mice deficient in recombination activating gene 2 by s.c. flank inoculation of 5×10^6 C6 glioma cells in 100 μl PBS supplemented with 0.1% glucose (16). When tumors had reached a volume of 350–450 mm^3, animals were assigned randomly to the various groups and injected intratumorally for up to 8 days with 50 μg/day JWH-133 and/or 60 μg/day fumonisin B1 (Alexis, San Diego, CA). Control animals were injected with vehicle. Tumors were measured with external caliper, and volume was calculated as $(4\pi/3) \times (\text{width}/2)^2 \times (\text{length}/2)$.

Human Tumor Samples. Tumor biopsies were obtained from two of the patients enrolled in an ongoing Phase I/II clinical trial (at the Neurosurgery Department of Tenerife University Hospital, Spain) aimed at investigating the effect of Δ^9-tetrahydrocannabinol administration on the growth of recurrent glioblastoma multiforme. The patients had failed standard therapy, which included surgery, radiotherapy (60 Gy), and temozolomide chemotherapy (4 cycles). Patients had clear evidence of tumor progression on sequential magnetic resonance scanning before enrollment in the study, had received no anticancer therapy for ~1 year, and had a fair health status (Karnofski performance score = 90). The patients provided written informed consent. The protocol was approved by the Clinical Trials Committee of Tenerife University Hospital and by the Spanish Ministry of Health.

Patient 1 (a 48-year-old man) had a right-occipital-lobe tumor (7.5 × 6 cm maximum diameters), and Patient 2 (a 57-year-old-man) had a right-temporal-lobe tumor (6 × 5 cm maximum diameters). Both tumors were diagnosed by the Pathology Department of Tenerife University Hospital as glioblastoma multiforme and showed the hallmarks of this type of tumor (high vascularization, necrotic areas, abundant palisading and mitotic cells, and so on). The tumors were removed extensively by surgery, biopsies were taken, and the tip (~5 cm) of a silastic infusion cathether (9.6 French; 3.2 mm diameter) was placed into the resection cavity. The infusion cathether was connected to a Nuport subclavicular s.c. reservoir. Each day 0.5–1.5 (median 1.0) mg of Δ^9-tetrahydrocannabinol (100 μg/μl in ethanol solution) were dissolved in 30 ml of physiological saline solution supplemented with 0.5% (w/v) human serum albumin, and the resulting solution was filtered and subsequently administered at a rate of 0.3 ml/min with a syringe pump connected to the s.c. reservoir. Patient 1 started the treatment 4 days after the surgery and received a total amount of 24.5 mg of Δ^9-tetrahydrocannabinol for 19 days. The posttreatment biopsy was taken 19 days after the cessation of Δ^9-tetrahydrocannabinol administration. Patient 2 started the treatment 4 days after the surgery and received a total amount of 13.5 mg of Δ^9-tetrahydrocannabinol for 16 days. The posttreatment biopsy was taken 43 days after the cessation of Δ^9-tetrahydrocannabinol administration. Samples were either transferred to DMEM containing 15% FCS and 1 mM glutamine (for tumor-cell isolation, see above; Fig. 2*B*) and frozen (for VEGF determination, Patients 1 and 2; and for VEGFR-2 Western blotting, Patient 1; Fig. 6, *A* and *C*) or fixed in formalin and embedded in paraffin (for VEGFR-2 confocal microscopy, Patients 1 and 2; Fig. 6*B*).

The cDNA Arrays. Total RNA was extracted (27) from tumors of vehicle- or JWH-133-treated mice (see above), and poly(A)$^+$ RNA was isolated with oligotex resin (Qiagen Inc., Valencia, CA) and reverse-transcribed with Moloney murine leukemia virus reverse transcriptase in the presence of 50 μCi [α-^{33}P]dATP for the generation of radiolabeled cDNA probes. Purified radiolabeled probes were hybridized to angiogenesis, hypoxia, and metastasis gene array membranes (GEArray Q Series; Superarray Bioscience Corporation, Frederick, MD) according to the manufacturer's instructions.[5] Hybridization signals were detected by phosphorimager and analyzed by Phoretix housekeeping genes in the blots as internal controls for normalization. The selection criteria were set conservatively throughout the process, and the genes selected were required to exhibit at least a 2-fold change of expression and a $P < 0.01$.

ELISA. VEGF levels were determined in cell culture media and in tumor extracts, obtained by homogenization as described previously (16), by solid-phase ELISA using the Quantikine mouse VEGF Immunoassay (R&D Systems, Abingdon, United Kingdom; 70% cross-reactivity with rat VEGF) for rat and mouse samples and the Quantikine human VEGF Immunoassay (R&D Systems) for human samples.

Western Blot. Particulate cell or tissue fractions were subjected to SDS-PAGE, and proteins were transferred from the gels onto polyvinylidene fluoride membranes. Blots were incubated with antibodies against total VEGFR-2 (1:1000; Santa Cruz Biotechnology, Santa Cruz, CA), VEGFR-2 phosphotyrosine 996 (1:250; Cell Signaling, Beverly, MA), VEGFR-2 phosphotyrosine 1214 (1:250; kindly given by Dr. Francesco Pezzella, Nuffield Department of Clinical Laboratory Science, University of Oxford, United Kingdom), and α-tubulin (1:4000, Sigma). The latter was used as a loading control. In all of the cases, samples were subjected to luminography with an enhanced chemiluminescence detection kit (Amersham Life Sciences, Arlington Heights, IL). Densitometric analysis of the blots was performed with the Multianalyst software (Bio-Rad Laboratories, Hercules, CA).

Confocal Microscopy. Glioma cells were cultured in coverslips and fixed in acetone for 10 min. Mouse tumors were dissected and frozen, and 5-μm sections were fixed in acetone for 10 min. Human tumors were fixed in 10% buffered formalin and then paraffin-embedded, 5-μm sections were deparaffinized and rehydrated, and antigen retrieval was carried out by immersing the slides in 10 mM citrate (pH 6.0) and boiling for 3 min. All of the samples were incubated with 10% goat serum in PBS for 30 min at room temperature to block nonspecific binding. Slices were incubated for 1.5 h with the aforementioned primary antibodies against total VEGFR-2 (1:50) and VEGFR-2 phosphotyrosine 1214 (1:20). After washing with PBS, slices were additionally incubated (1 h, room temperature, darkness) with a mixture of the secondary goat antimouse antibodies Alexa Fluor 488 and Alexa Fluor 546 (both at 1:400; Molecular Probes, Leyden, The Netherlands). After washing with PBS, sections were fixed in 1% paraformaldehyde for 10 min and mounted with DAKO fluorescence mounting medium containing TOTO-3 iodide (1:1000; Molecular Probes) to stain cell nuclei. Confocal fluorescence images were acquired using a Laser Sharp 2000 software (Bio-Rad) and a Confocal Radiance 2000 coupled to Axiovert S100 TV microscope (Carl Zeiss, Oberkochen, Germany). Pixel quantification and colocalization were determined with Metamorph-Offline software (Universal Imaging, Downingtown, PA).

Ceramide Synthesis. C6 glioma cells were cultured for 48 h in serum-free medium with the additions indicated together with 1 μCi of L-U-[^{14}C]serine/well, lipids were extracted, and ceramide resolved by thin-layer chromatography as described previously (28).

Statistics. Results shown represent mean ± SD. Statistical analysis was performed by ANOVA with a *post hoc* analysis by the Student-Neuman-Keuls test or by unpaired Student's *t* test.

RESULTS

Changes in Gene Expression Profile in Mouse Gliomas. The cDNA array analysis was used as a first approach to test whether cannabinoid administration affects the VEGF pathway in mouse gliomas. Because cannabinoid-based therapeutic strategies should be as devoid as possible of psychotropic side effects and glioma cells express functional CB_2 receptors, which do not mediate psychoactivity (16, 26), mice bearing s.c. gliomas were injected with the selective CB_2 agonist JWH-133 (26).

A total of 267 genes related to angiogenesis, hypoxia (perhaps the most potent stimulus for the onset of tumor angiogenesis), and metastasis (a characteristic of actively growing tumors related closely to angiogenesis) were analyzed, of which 126 were considered to be expressed in reliable amounts. JWH-133 administration altered the expression of 10 genes, all of which are directly or indirectly related to the VEGF pathway (Fig. 1). Thus, cannabinoid treatment lowered the expression of the following: (*a*) VEGF-A [confirming our previous Northern blot data (22)] and its relative VEGF-B (3, 4); (*b*) hypoxia-inducible factor-1α [one of the subunits of hypoxia-inducible factor-1, the major transcription factor involved in VEGF gene expression (29)]; (*c*) two genes known to be under the control of VEGF, namely those encoding connective tissue growth factor [a mitogen involved in extracellular matrix production and angiogenesis (30)], and heme oxygenase-1 [an enzyme highly expressed during hypoxia and inflammation (31)]; and (*d*) four genes known to encode proteins functionally related to VEGF, namely Id3 [a transcription factor inhibitor involved in angiogenesis and tumor progression (32)], midkine [a proangiogenic and tumorigenic growth factor (33)], angiopoi-

[5] See Internet address http://www.superarray.com for a detailed list of the genes analyzed.

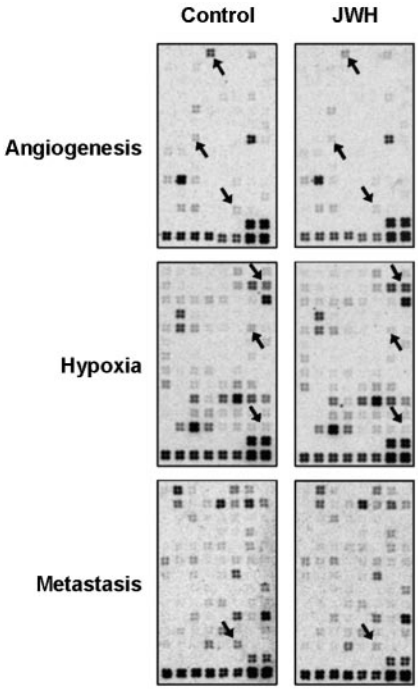

Gene name	JWH effect (Control = 1.0)
VEGF-A	0.5
VEGF-B	0.2
Hypoxia-inducible factor-1α	0.4
Connective tissue growth factor	0.4
Heme oxygenase-1	0.5
Id 3	0.4
Midkine	0.5
Angiopoietin-2	0.5
Tie-1	0.4
Procollagen Iα1	2.1

Fig. 1. Changes in gene expression profile in mouse gliomas after cannabinoid treatment. Animals bearing gliomas were treated with either vehicle (*Control*) or JWH-133 (*JWH*) for 8 days as described in "Materials and Methods." Equal amounts of poly(A)$^+$ RNA from tumors of 2 animals/group were pooled and hybridized to angiogenesis, hypoxia, and metastasis cDNA array membranes. Genes affected by cannabinoid treatment are listed. Examples of affected genes are pointed with *arrows*. Angiogenesis membrane, angiopoietin-2 (*top*), midkine (*middle*), and VEGF-A (*bottom*); Hypoxia membrane, procollagen Iα1 (*top*), heme oxygenase-1 (*middle*), and VEGF-A (*bottom*); and Metastasis membrane, VEGF-A.

etin-2 [a prominent proangiogenic factor that cooperates with VEGF (3, 19, 22)], and Tie-1 [an angiopoietin receptor (34)]. In addition, cannabinoid treatment increased the expression of the gene encoding type I procollagen α1 chain (a metalloproteinase substrate related to matrix remodeling during angiogenesis; Ref. 35).

Inhibition of VEGF Production in Cultured Glioma Cells and in Mouse Gliomas. We focused next on the two main components of the VEGF pathway, namely VEGF and VEGFR-2, in both cultured glioma cells and gliomas *in vivo*. Incubation of C6 glioma cells with the synthetic cannabinoid WIN-55,212-2 (100 nM), a mixed CB_1/CB_2

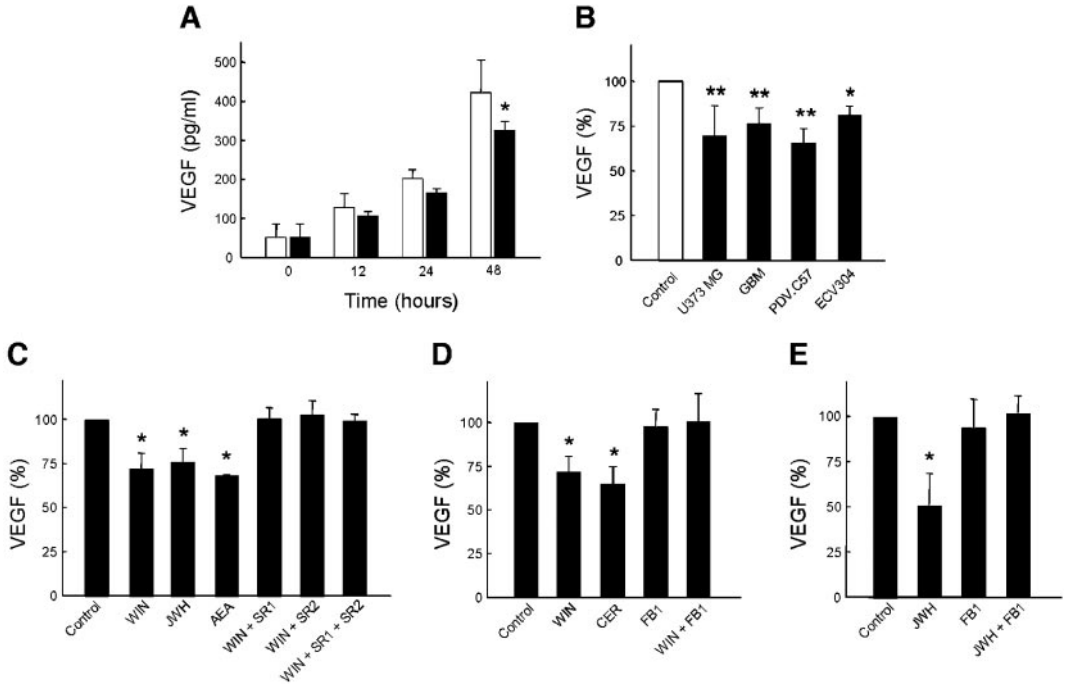

Fig. 2. Inhibition of VEGF production by cannabinoids in cultured glioma cells and in mouse gliomas. *A*, C6 glioma cells were cultured for the times indicated with vehicle (□) or 100 nM WIN-55,212-2 (■), and VEGF levels in the medium were determined ($n = 4$). *B*, U373 MG astrocytoma cells, tumor cells obtained from a patient with glioblastoma multiforme (*GBM*), PDV.C57 epidermal carcinoma cells, and ECV304 bladder cancer epithelioma cells were cultured for 48 h with vehicle (□) or 100 nM WIN-55,212-2 (■), and VEGF levels in the medium were determined. Data represent the percentage of VEGF in cannabinoid incubations *versus* the respective controls ($n = 3$–4). *C*, C6 glioma cells were cultured for 48 h with vehicle (*Control*), 100 nM WIN-55,212-2 (*WIN*), 100 nM JWH-133 (*JWH*), 2 μM anandamide (*AEA*), 0.5 μM SR141716 (*SR1*), and/or 0.5 μM SR144528 (*SR2*), and VEGF levels in the medium were determined ($n = 4$–6). *D*, C6 glioma cells were cultured for 48 h with vehicle (*Control*), 100 μM WIN-55, 212-2 (*WIN*), 1 μM C_2-ceramide (*CER*), and/or 0.5 μM fumonisin B1 (*FB1*), and VEGF levels in the medium were determined ($n = 4$). *E*, animals bearing gliomas were treated with either vehicle (*Control*), JWH-133 (*JWH*), fumonisin B1 (*FB1*), or JWH-133 plus fumonisin B1 for 8 days as described in "Materials and Methods," and VEGF levels in the tumors were determined ($n = 4$–6 for each experimental group). Significantly different (*, $P < 0.01$; **, $P < 0.05$) from control incubations or control animals. *Bars*, ±SD.

receptor agonist, inhibited VEGF release into the medium in a time-dependent manner (Fig. 2*A*). The cannabinoid did not affect cell viability throughout the time interval in which VEGF determinations were performed (up to 48 h; data not shown). Cannabinoid-induced attenuation of VEGF production was evident in another glioma cell line (the human astrocytoma U373 MG) and, more importantly, in tumor cells obtained directly from a human glioblastoma multiforme biopsy (Fig. 2*B*). The cannabinoid effect was also observed in the mouse skin carcinoma PDV.C57 and in the human bladder cancer epithelioma ECV304 (Fig. 2*B*).

To prove the specificity of WIN-55,212-2 action on VEGF release, we used other cannabinoid receptor agonists as well as selective cannabinoid receptor antagonists (Fig. 2*C*). The inhibitory effect of WIN-55,212-2 was mimicked by the endocannabinoid anandamide (2 μM), another mixed CB_1/CB_2 agonist, and by the synthetic cannabinoid JWH-133 (100 nM), a selective CB_2 agonist. In addition, the CB_1 antagonist SR141716 (0.5 μM) and the CB_2 antagonist SR144528 (0.5 μM) prevented WIN-55,212-2 action, pointing to the involvement of CB receptors in cannabinoid-induced inhibition of VEGF production.

The sphingolipid messenger ceramide has been implicated in the regulation of tumor cell function by cannabinoids (16, 23, 36). The involvement of ceramide in cannabinoid-induced inhibition of VEGF production was tested by the use of *N*-acetylsphingosine (C_2-ceramide), a cell-permeable ceramide analog, and fumonisin B1, a selective inhibitor of ceramide synthesis *de novo*. In line with our previous data in primary cultures of rat astrocytes (28), fumonisin B1 was able to prevent cannabinoid-induced ceramide biosynthesis (relative values of [^{14}C]serine incorporation into ceramide, $n = 3$: vehicle, 100; 100 nM WIN-55,212-2, 140 $\pm$ 1; 100 nM WIN-55,212-2 plus 0.5 μM fumonisin B1, 86 $\pm$ 9). C_2-ceramide (1 μM) depressed VEGF production, whereas pharmacological blockade of ceramide synthesis *de novo* with fumonisin B1 (0.5 μM) prevented the inhibitory effect of WIN-55,212-2 (Fig. 2*D*). We subsequently evaluated whether fumonisin B1 action was also evident *in vivo*. The decrease in tumor VEGF levels induced by cannabinoid administration (19, 22, 37) was prevented by cotreatment of the animals with fumonisin B1 (Fig. 2*E*).

Inhibition of VEGFR-2 in Cultured Glioma Cells and in Mouse Gliomas. VEGFR-2 activation was determined by measuring the extent of phosphorylation of two of its essential tyrosine autophosphorylation residues, namely 996 and 1214 (3, 4). Western blot experiments showed that C6 glioma cells express highly phosphorylated VEGFR-2 in the absence of ligand, indicating that the receptor may be constitutively active. Incubation of C6 glioma cells with WIN-55,212-2 or JWH-133 decreased VEGFR-2 activation without affecting total VEGFR-2 levels (Fig. 3*A*). Confocal microscopy experiments confirmed the decrease in VEGFR-2 immunoreactivity by cannabinoid challenge when fluorescence was expressed per cell nucleus (Fig. 3*B*) or per total-VEGFR-2 fluorescence (data not shown). Moreover, fumonisin B1 prevented cannabinoid inhibitory action, and C_2-ceramide reduced VEGFR-2 activation (Fig. 3, *A* and *B*). Interestingly, on cannabinoid exposure the receptor seemed to be preferentially condensed in the perinuclear region, and this relocalization was prevented by fumonisin B1 (Fig. 3*B*). The functional impact of VEGF on C6 glioma cells was supported by the finding that VEGF induced a prosurvival action by preventing the loss of cell viability on prolonged (72 h) cannabinoid or C_2-ceramide challenge (Fig. 3*C*).

The effect of cannabinoid administration on VEGFR-2 activation was subsequently tested in tumor-bearing mice. The ceramide-dependent cannabinoid-induced inhibition of VEGFR-2 activation found in cultured cells was also observed by Western blot (Fig. 4*A*) and confocal microscopy (Fig. 4*B*) in mouse gliomas. Like in the cultured-cell experiments and in line with the cDNA array experiments (data not shown), total VEGFR-2 expression in the tumors was unaffected by cannabinoid treatment (Fig. 4, *A* and *B*).

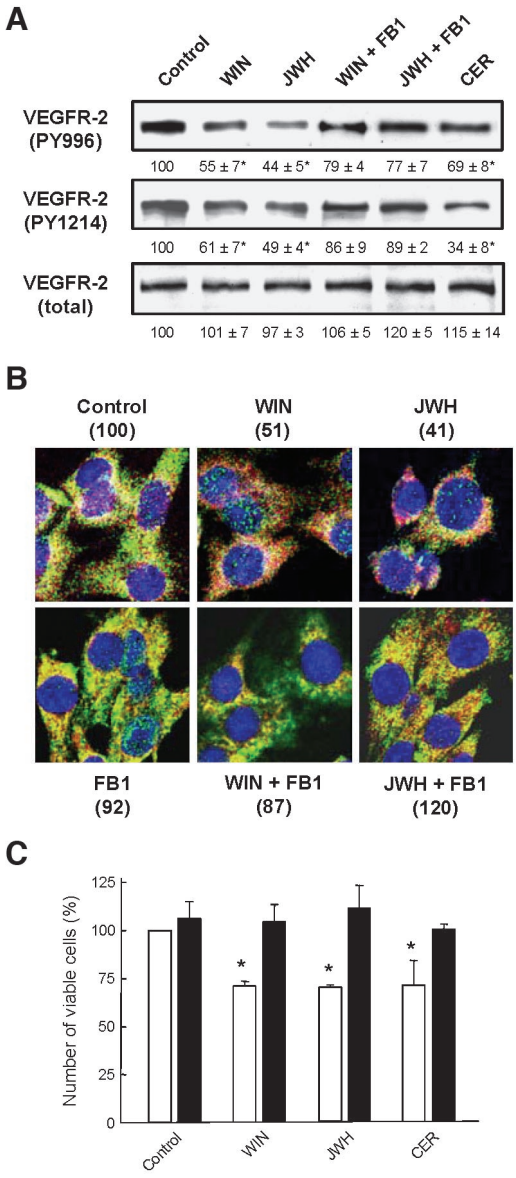

Fig. 3. Inhibition of VEGFR-2 by cannabinoids in cultured glioma cells. *A*, C6 glioma cells were cultured for 4 h with vehicle (*Control*), 100 nM WIN-55,212-2 (*WIN*), 100 nM JWH-133 (*JWH*), 10 μM C_2-ceramide (*CER*), and/or 0.5 μM fumonisin B1 (*FB1*), and VEGFR-2 activation (anti-*VEGFR-2 PY996* and anti-*VEGR2 PY1214* antibodies) and expression (antitotal *VEGFR-2* antibody) were determined by Western blot. Absorbance values relative to those of total VEGFR-2 are given in arbitrary units. Significantly different (*, $P < 0.01$) from control incubations ($n = 3$). *B*, C6 glioma cells were cultured as in panel *A*, and VEGFR-2 activation (anti-VEGFR-2 PY1214 antibody, *green*) and expression (antitotal VEGFR-2 antibody, *red*) were determined by confocal microscopy. Cell nuclei are stained in *blue*. One representative experiment of 3 is shown. Relative values of activated-VEGFR-2 pixels/cell nucleus are given in parentheses. *C*, C6 glioma cells were cultured for 72 h with vehicle (*Control*), 100 nM WIN-55,212-2 (*WIN*), 100 nM JWH-133 (*JWH*), or 1 μM C_2-ceramide (*CER*) with (■) or without (□) 50 ng/ml VEGF, and the number of viable cells was determined. Significantly different (*, $P < 0.01$) from control incubations ($n = 3$–4). *Bars*, ±SD.

Phosphorylated VEGFR-2 has been found previously in the cell nucleus, and it has been postulated that this translocation process might play a role in VEGFR-2 signaling (38–40). However, by confocal microscopy, we found a rather variable fraction of phosphorylated VEGFR-2 in the nuclei of C6 glioma cells in culture and on inoculation in mice, and this fraction of nuclear VEGFR-2 was unaltered after treatment with cannabinoids and/or fumonisin B1 *in vitro* and *in vivo* (data not shown).

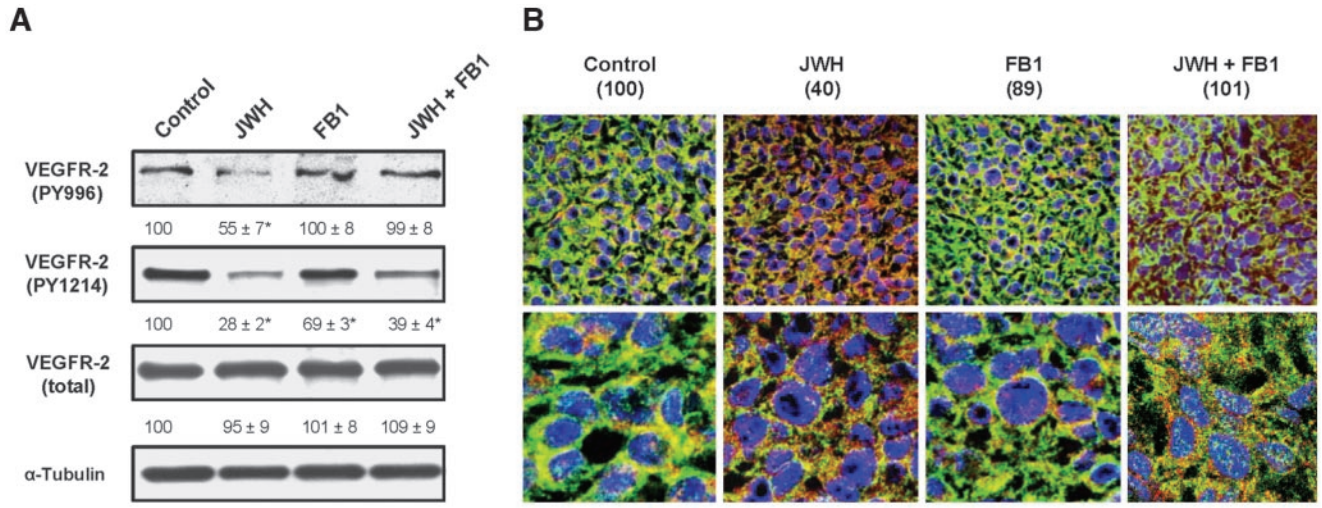

Fig. 4. Inhibition of VEGFR-2 by cannabinoids in mouse gliomas. *A*, animals bearing gliomas were treated with either vehicle (*Control*), JWH-133 (*JWH*), fumonisin B1 (*FB1*), or JWH-133 plus fumonisin B1 for 8 days as described in "Materials and Methods," and VEGFR-2 activation (anti-*VEGFR-2 PY996* and anti-*VEGR2 PY1214* antibodies) and expression (antitotal *VEGFR-2* antibody) were determined by Western blot. Absorbance values relative to those of total VEGFR-2 (phosphorylated VEGFR-2 blots) or of α-tubulin (total VEGFR-2 blots) are given in arbitrary units. Significantly different (*, $P < 0.01$) from control animals ($n = 3$–4 for each experimental group). *B*, animals bearing gliomas were treated as in panel *A*, and VEGFR-2 activation (anti-VEGFR-2 1214 antibody, *green*) and expression (antitotal VEGFR-2 antibody, *red*) were determined by confocal microscopy. Cell nuclei are stained in *blue*. Low- and high-magnification pictures are shown. One representative tumor of 3–4 for each experimental group is shown. Relative values of activated-VEGFR-2 pixels/cell nucleus are given in parentheses.

Changes in the Size of Mouse Gliomas. To test whether the aforementioned ceramide-dependent changes in the VEGF pathway are functionally relevant, we measured tumor size along cannabinoid and fumonisin B1 treatment. In agreement with previous observations (26), JWH-133 administration blocked the growth of s.c. gliomas in mice. Of importance, cotreatment of the animals with fumonisin B1 prevented cannabinoid antitumoral action (Fig. 5).

Inhibition of the VEGF Pathway in Two Patients with Glioblastoma Multiforme. To obtain additional support for the potential therapeutic implication of cannabinoid-induced inhibition of the VEGF pathway, we analyzed the tumors of two patients enrolled in a clinical trial aimed at investigating the effect of Δ^9-tetrahydrocannabinol, a mixed CB_1/CB_2 agonist, on recurrent glioblastoma multiforme. The patients were subjected to local Δ^9-tetrahydrocannabinol administration, and biopsies were taken before and after the treatment. In both patients, VEGF levels in tumor extracts were lower after cannabinoid inoculation (Fig. 6*A*). The Δ^9-tetrahydrocannabinol also lowered the expression of phosphorylated VEGFR-2 in the tumors of the two patients, and this was accompanied (in contrast to the mouse glioma experiments shown above) by a decrease in total VEGFR-2 levels (Fig. 6*B*). This was confirmed by Western blot analysis in Patient 1 (Fig. 6*C*). Unfortunately, we were unable to obtain appropriate samples for Western blot from Patient 2.

DISCUSSION

Angiogenesis is a prerequisite for the progression of most solid tumors. In particular, gliomas first acquire their blood supply by co-opting existing normal brain vessels to form a well-vascularized tumor mass without the necessity to initiate angiogenesis (41–43). When gliomas progress, they become hypoxic as the co-opted vasculature regresses and malignant cells rapidly proliferate. These hypoxic conditions, in turn, induce robust angiogenesis via the VEGF pathway and angiopoietin-2, and in fact, this angiogenic sprouting distinguishes a grade IV astrocytoma (glioblastoma multiforme) from lower-grade astrocytomas (41–43). Here, we show that cannabinoid treatment impairs the VEGF pathway in mouse gliomas by blunting VEGF production and signaling. Cannabinoid-induced inhibition of VEGF expression and VEGFR-2 activation also occurred in cultured glioma cells, indicating that the changes observed *in vivo* may reflect the direct impact of cannabinoids on tumor cells. Moreover, a depression of the VEGF pathway was also evident in two patients with glioblastoma multiforme. Although the changes in VEGFR-2 expression observed in these two patients

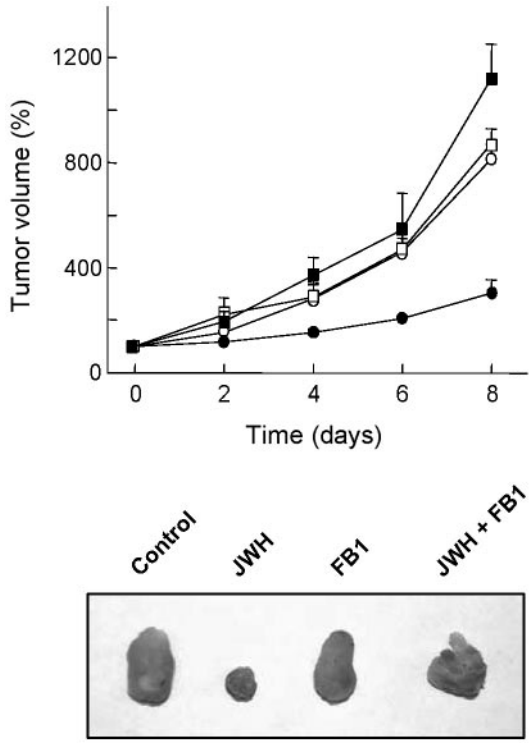

Fig. 5. Changes in the size of mouse gliomas after cannabinoid and fumonisin B1 treatment. Animals bearing gliomas ($n = 4$–6 for each experimental group) were treated with either vehicle (*Control*, ○), JWH-133 (*JWH*, ●), fumonisin B1 (*FB1*, □), or JWH-133 plus fumonisin B1 (■) for up to 8 days as described in "Materials and Methods." Examples of formaldehyde-fixed dissected tumors after 8 days of treatment are shown. *Bars*, ±SD.

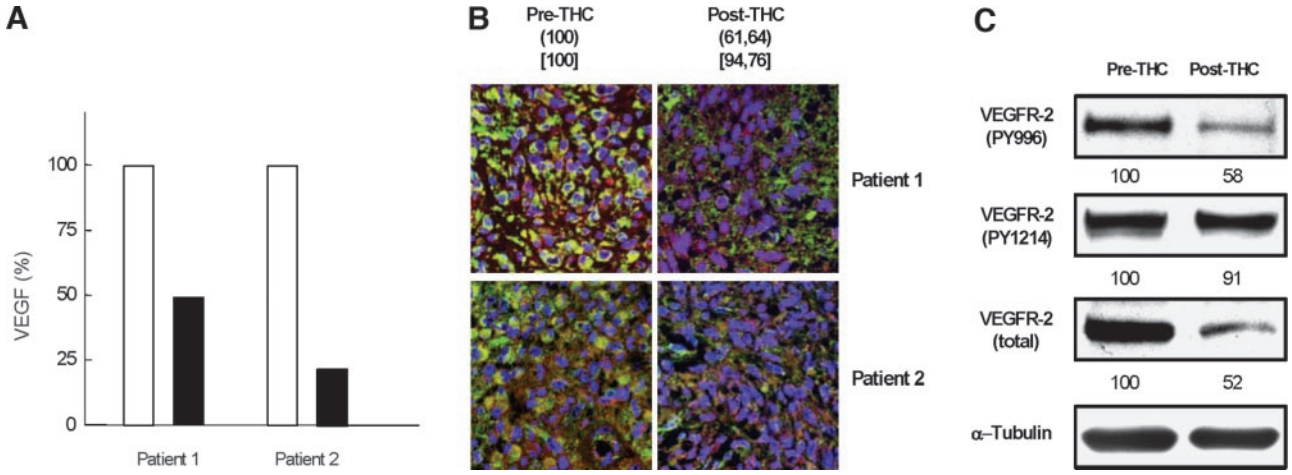

Fig. 6. Inhibition of the VEGF pathway in two patients with glioblastoma multiforme after cannabinoid treatment. The patients were subjected to Δ^9-tetrahydrocannabinol (*THC*) administration as described in "Materials and Methods." *A*, VEGF levels in the tumors before (□) and after (■) THC treatment. *B*, VEGFR-2 activation (anti-VEGFR-2 PY1214 antibody, *green*) and expression (antitotal VEGFR-2 antibody, *red*) in the tumors before and after THC treatment as determined by confocal microscopy. Cell nuclei are stained in *blue*. Relative values of activated-VEGFR-2 pixels (*parentheses*) and of total-VEGFR-2 pixels (*square brackets*) per cell nucleus are given for the two patients. *C*, VEGFR-2 activation (anti-*VEGFR-2 PY996* and anti-*VEGR2 PY1214* antibodies) and expression (antitotal *VEGFR-2* antibody) in the tumor of Patient 1 before and after THC treatment, as determined by Western blot. Absorbance values relative to those of loading controls (α-tubulin) are given in arbitrary units.

do not fully mirror the cultured-cell and mouse data, they clearly follow the same direction. The molecular basis of this discrepancy is, however, unknown.

Our observations do not exclude that cannabinoids may also blunt tumor VEGF signaling indirectly by targeting other receptor-mediated processes that stimulate the VEGF pathway. For example, it is known that engagement of epidermal growh factor (44) and nerve growth factor (45) receptors induces the VEGF pathway, and cannabinoids have been reported to inhibit the epidermal growth factor receptor in skin carcinoma (19) and prostate carcinoma cells (46) as well as the TrkA neurotrophin receptor in breast carcinoma (47) and pheochromocytoma cells (20). However, the molecular mechanisms by which cannabinoid receptor activation impact these growth factor receptors remain obscure.

Recent work has shown that cannabinoids can modulate sphingolipid-metabolizing pathways by increasing the intracellular levels of ceramide (23), a lipid second messenger that controls cell fate in different systems (48, 49). After cannabinoid receptor activation, two peaks of ceramide generation are observed in glioma cells that have different mechanistic origin: (*a*) the first peak comes from sphingomyelin hydrolysis (50); and (*b*) the second peak originates from ceramide synthesis *de novo* (36). The findings reported here expand the role of *de novo*-synthesized ceramide in cannabinoid action. Moreover, as far as we know, this is also the first report showing that ceramide depresses the VEGF pathway by interfering with VEGF production and VEGFR-2 activation, a notion that is in line with the observation that ceramide analogs prevent VEGF-induced cell survival (51, 52). In the context of the "sphingolipid rheostat" theory (48, 49), the mitogenic sphingolipid sphingosine 1-phosphate would shift the balance toward angiogenesis and tumorigenesis (5, 53), whereas the antiproliferative sphingolipid ceramide would blunt angiogenesis and tumorigenesis (present study).

The use of cannabinoids in medicine is limited by their psychoactive effects mediated by neuronal CB_1 receptors (9, 10). Although these adverse effects are within the range of those accepted for other medications, especially in cancer treatment, and tend to disappear with tolerance on continuous use (20), it is obvious that cannabinoid-based therapies devoid of side-effects would be desirable. As glioma cells express functional CB_2 receptors (26), we used a selective CB_2 ligand to target the VEGF pathway. Selective CB_2 receptor activation in mice also inhibits the growth and angiogenesis of skin carcinomas (19). Unfortunately, very little is known about the pharmacokinetics and toxicology of the selective CB_2 ligands synthesized to date, making them as yet unavailable for clinical trials.

Gliomas are one of the most malignant forms of cancer, resulting in the death of affected patients within 1–2 two years after diagnosis. Current therapies for glioma treatment are usually ineffective or just palliative. Therefore, it is essential to develop new therapeutic strategies for the management of glioblastoma multiforme, which will most likely require a combination of therapies to obtain significant clinical results. In line with the idea that anti-VEGF treatments constitute one of the most promising antitumoral approaches currently available (5–7), the present laboratory and clinical findings provide a novel pharmacological target for cannabinoid-based therapies.

ACKNOWLEDGMENTS

We are indebted to M. A. Muñoz and C. Sánchez for expert technical assistance in the confocal microscopy experiments, Dr. L. García for personal support, and Drs. G. Velasco and I. Galve-Roperh for discussion and advice.

REFERENCES

1. Carmeliet P. Angiogenesis in health and disease. Nat Med 2003;9:653–60.
2. Bergers G, Benjamin LE. Tumorigenesis and the angiogenic switch. Nat Rev Cancer 2003;3:401–10.
3. Yancopoulos GD, Davis S, Gale NW, et al. Vascular-specific growth factors and blood vessel formation. Nature (Lond) 2000;407:242–8.
4. Ferrara N, Gerber HP, LeCouter J. The biology of VEGF and its receptors. Nat Med 2003;9:669–76.
5. Kerbel R, Folkman J. Clinical translation of angiogenesis inhibitors. Nat Rev Cancer 2002;2:727–39.
6. Huang J, Frischer JS, Serur A, et al. Regression of established tumors and metastases by potent vascular endothelial growth factor blockade. Proc Natl Acad Sci USA 2003;100:7785–90.
7. Willett CG, Boucher Y, di Tomaso E, et al. Direct evidence that the VEGF-specific antibody bevacizumab has antivascular effects in human rectal cancer. Nat Med 2004;10:145–7.
8. Sausville EA, Elsayed Y, Monga M, Kim G. Signal transduction-directed cancer treatments. Annu Rev Pharmacol Toxicol 2003;43:199–231.
9. Howlett AC, Barth F, Bonner TI, et al. International Union of Pharmacology. XXVII. Classification of cannabinoid receptors. Pharmacol Rev 2002;54:161–202.
10. Piomelli D. The molecular logic of endocannabinoid signalling. Nat Rev Neurosci 2003;4:873–84.
11. Tramer MR, Carroll D, Campbell FA, et al. Cannabinoids for control of chemotherapy induced nausea and vomiting: quantitative systematic review. BMJ 2001;323:16–21.

12. Walker J, Huang S. Cannabinoid analgesia. Pharmacol Ther 2002;95:127–35.
13. Zajicek J, Fox P, Sanders H, et al. Cannabinoids for treatment of spasticity and other symptoms related to multiple sclerosis (CAMS study): multicentre randomised placebo-controlled trial. Lancet 2003;362:1517–26.
14. Mechoulam R, Panikashvili D, Shohami E. Cannabinoids and brain injury: therapeutic implications. Trends Mol Med 2002;8:58–61.
15. Munson AE, Harris LS, Friedman MA, Dewey WL, Carchman RA. Antineoplastic activity of cannabinoids. J Natl Cancer Inst (Bethsda) 1975;55:597–602.
16. Galve-Roperh I, Sánchez C, Cortés ML, et al. Antitumoral action of cannabinoids: involvement of sustained ceramide accumulation and extracellular signal-regulated kinase activation. Nat Med 2000;6:313–9.
17. Bifulco M, Laezza C, Portella G, et al. Control by the endogenous cannabinoid system of ras oncogene-dependent tumor growth. FASEB J 2001;15:2745–7.
18. McKallip RJ, Lombard C, Fisher M, et al. Targeting CB2 cannabinoid receptors as a novel therapy to treat malignant lymphoblastic disease. Blood 2002;100:627–34.
19. Casanova ML, Blázquez C, Martínez-Palacio J, et al. Inhibition of skin tumor growth and angiogenesis in vivo by activation of cannabinoid receptors. J Clin Investig 2003;111:43–50.
20. Guzmán M. Cannabinoids: potential anticancer agents. Nat Rev Cancer 2003;3:745–55.
21. Bifulco M, Di Marzo V. Targeting the endocannabinoid system in cancer therapy: a call for further research. Nat Med 2002;8:547–50.
22. Blázquez C, Casanova ML, Planas A, et al. Inhibition of tumor angiogenesis by cannabinoids. FASEB J 2003;17:529–31.
23. Guzmán M, Galve-Roperh I, Sánchez C. Ceramide: a new second messenger of cannabinoid action. Trends Pharmacol Sci 2001;22:19–22.
24. Huffman JW, Liddle J, Yu S, et al. 3-(1′,1′-Dimethylbutyl)-1-deoxy-delta-8-Δ^9-tetrahydrocannabinol and related compounds: synthesis of selective ligands for the CB_2 receptor. Bioorg Med Chem Lett 1999;7:2905–14.
25. Sánchez C, Galve-Roperh I, Canova C, Brachet P, Guzmán M. Δ^9-Tetrahydrocannabinol induces apoptosis in C6 glioma cells. FEBS Lett 1988;436:6–10.
26. Sánchez C, de Ceballos ML, Gómez del Pulgar T, et al. Inhibition of glioma growth in vivo by selective activation of the CB_2 cannabinoid receptor. Cancer Res 2001; 61:5784–9.
27. Casanova ML, Larcher F, Casanova B, et al. A critical role for ras-mediated, EGFR-dependent angiogenesis in mouse skin carcinogenesis. Cancer Res 2002;62: 3402–7.
28. Blázquez C, Galve-Roperh I, Guzmán, M. De novo-synthesized ceramide signals apoptosis in astrocytes via extracellular signal-regulated kinase. FASEB J 2000;14: 2315–22.
29. Pugh CW, Ratcliffe PJ. Regulation of angiogenesis by hypoxia: role of the HIF system. Nat Med 2003;9:677–84.
30. Suzuma K, Naruse K, Suzuma I, et al. Vascular endothelial growth factor induces expression of connective tissue growth factor via KDR, Flt1, and phosphatidylinositol 3-kinase-akt-dependent pathways in retinal vascular cells. J Biol Chem 2000;275: 40725–31.
31. Bussolati B, Ahmed A, Pemberton H, et al. Bifunctional role for VEGF-induced heme oxygenase-1 in vivo: induction of angiogenesis and inhibition of leukocyte infiltration. Blood 2004;103:761–6.
32. de Candia P, Solit DB, Giri D, et al. Angiogenesis impairment in Id-deficient mice cooperates with a Hsp90 inhibitor to completely suppress HER2/neu-dependent breast tumors. Proc Natl Acad Sci USA 2003;100:12337–432.
33. Barthlen W, Flaadt D, Girgert R, et al. Significance of heparin-binding growth factor expression on cells of solid pediatric tumors. J Pediatr Surg 2003;38:1296–304.
34. Sato T, Qin Y, Kozak CA, Audus KL. Tie-1 and tie-2 define another class of putative receptor tyrosine kinase genes expressed in early embryonic vascular system. Proc Natl Acad Sci USA 1993;90:9355–8.
35. Seandel M, Noack-Kunnmann K, Zhu D, Aimes RT, Quigley JP. Growth factor-induced angiogenesis in vivo requires specific cleavage of fibrillar type I collagen. Blood 2001;97:2323–32.
36. Gómez del Pulgar T, Velasco G, Sánchez C, Haro A, Guzmán M. De novo-synthesized ceramide is involved in cannabinoid-induced apoptosis. Biochem J 2002; 363:183–8.
37. Portella G, Laezza C, Laccetti P, et al. Inhibitory effects of cannabinoid CB_1 receptor stimulation on tumor growth and metastatic spreading: actions on signals involved in angiogenesis and metastasis. FASEB J 2003;17:1771–3.
38. Feng Y, Venema VJ, Venema RC, Tsai N, Caldwell RB. VEGF induces nuclear translocation of Flk-1/KDR, endothelial nitric oxide synthase, and caveolin-1 in vascular endothelial cells. Biochem Biophys Res Commun 1999;256:192–7.
39. Dougher M, Terman BI. Autophosphorylation of KDR in the kinase domain is required for maximal VEGF-stimulated kinase activity and receptor internalization. Oncogene 1999;18:1619–27.
40. Stewart M, Turley H, Cook N, et al. The angiogenic receptor KDR is widely distributed in human tissues and tumours and relocates intracellularly on phosphorylation. An immunohistochemical study. Histopathology 2003;43:33–9.
41. Holash J, Maisonpierre PC, Compton D, et al. Vessel cooption, regression, and growth in tumors mediated by angiopoietins and VEGF. Science (Wash DC) 1999; 284:1994–8.
42. Zagzag D, Amirnovin R, Greco MA, et al. Vascular apoptosis and involution in gliomas precede neovascularization: a novel concept for glioma growth and angiogenesis. Lab Investig 2000;80:837–49.
43. Vajkoczy P, Farhadi M, Gaumann A, et al. Microtumor growth initiates angiogenic sprouting with simultaneous expression of VEGF, VEGF receptor-2, and angiopoietin-2. J Clin Investig 2002;109:777–85.
44. Goldman CK, Kim J, Wong WL, et al. Epidermal growth factor stimulates vascular endothelial growth factor production by human malignant glioma cells: a model of glioblastoma multiforme pathophysiology. Mol Biol Cell 1993;4:121–33.
45. Calza L, Giardino L, Giuliani A, Aloe L, Levi-Montalcini R. Nerve growth factor control of neuronal expression of angiogenetic and vasoactive factors. Proc Natl Acad Sci USA 2001;98:4160–5.
46. Mimeault M, Pommery N, Wattez N, Bailly C, Henichart JP. Anti-proliferative and apoptotic effects of anandamide in human prostatic cancer cell lines: implication of epidermal growth factor receptor down-regulation and ceramide production. Prostate 2003;56:1–12.
47. Melck D, Rueda D, Galve-Roperh I, et al. Involvement of the cAMP/protein kinase A pathway and of mitogen-activated protein kinase in the anti-proliferative effects of anandamide in human breast cancer cells. FEBS Lett 1999;463:235–40.
48. Hannun YA, Obeid LM. The ceramide-centric universe of lipid-mediated cell regulation: stress encounters of the lipid kind. J Biol Chem 2002;277:25847–50.
49. Kolesnick R. The therapeutic potential of modulating the ceramide/sphingomyelin pathway. J Clin Investig 2002;110:3–8.
50. Sánchez C, Rueda D, Segui B, et al. The CB_1 cannabinoid receptor of astrocytes is coupled to sphingomyelin hydrolysis through the adaptor protein fan. Mol Pharmacol 2001;59:955–9.
51. Gupta K, Kshirsagar S, Li W, et al. VEGF prevents apoptosis of human microvascular endothelial cells via opposing effects on MAPK/ERK and SAPK/JNK signaling. Exp Cell Res 1999;247:495–504.
52. Mesri M, Morales-Ruiz M, Ackermann EJ, et al. Suppression of vascular endothelial growth factor-mediated endothelial cell protection by survivin targeting. Am J Pathol 2001;158:1757–65.
53. Spiegel S, Milstien S. Sphingosine-1-phosphate: an enigmatic signalling lipid. Nat Rev Mol Cell Biol 2003;4:397–407.